

Measurement device and method for mass and centroid of large aircraft

ZHANG Xiaolin^{1*}, ZHANG Yuyang¹, YANG Lifeng², ZHAO Hongzhi², WANG Meibao³

1. School of Instrument Science and Engineering, Harbin Institute of Technology, Harbin 150006, China;

2. Capital Aerospace Machinery Co., Ltd., Beijing 100071, China;

3. School of Mechanical Engineering, Zhejiang Sci-Tech University, Hangzhou 310018, China

*Corresponding author: ZHANG Xiaolin (zhangxiaolin@hit.edu.cn)

Received: May 4, 2025

Revised: June 19, 2025

Accepted: July 10, 2025

Abstract: The precise acquisition of the quality characteristic parameters of large aircraft directly affects its performance characteristics. For large aircrafts such as missiles and rockets with internal fillings, traditional measurement methods involving large-angle tilting or rotation may pose safety risks. In light of the characteristics of large aircraft and in combination with existing measurement methods, we design a mass and centroid measurement method based on four-point support and small-angle tilting, and develop a set of mass and centroid testing system. This method obtains the intersection point of the gravity action line in the product coordinate system through coordinate transformation in two postures, thereby obtaining the three-dimensional centroid of the aircraft. We first elaborate on the principle of this method in detail, then introduce the composition of the equipment, and analyze the structural stress of key components. Finally, experimental verification and uncertainty analysis are carried out. Experimental verification shows that the maximum deviation of the mass measurement accuracy is less than 0.02%, the centroid measurement accuracy in the X direction is ± 0.15 mm, in the Y direction it is ± 0.21 mm, and in the Z direction it is ± 0.19 mm.

Key words: large aircraft; centroid measurement; coordinate transformation; multi-point weighing method; gravity line

0 Introduction

The precise acquisition of the quality characteristic parameters of large aircraft is of vital importance for its performance^[1,2]. The design of core algorithms in the flight control system as well as the force distribution of the propulsion system all requires the use of precise centroid coordinates as the calculation basis^[3-5].

In practical engineering applications, due to the influence of processing tolerances of components, cumulative errors during assembly, etc., it is difficult to precisely obtain the quality distribution characteristics of the aircraft solely through numerical simulation^[6]. Therefore, physical measurement methods must be employed for verification. Currently, the mainstream centroid measurement technologies mainly include multi-point weighing method^[7-9], torque balance method, compound pendulum measurement method, and suspension measurement method^[10,11]. Among them, the multi-point weighing system, with its advantages of high structural reliability, stable measurement accuracy, safe and convenient operation, can simultaneously obtain the quality and

centroid coordinate data. Thus, it has been widely applied in the field of measuring the quality characteristic parameters of large aircraft^[12].

The multi-point weighing system constructs a measurement platform by installing multiple force sensors. Based on the principle of static torque balance, the projection position of the centroid of the measured object in the platform coordinate system can be determined. By rotating or tilting the object to be measured at a certain angle, the projection coordinates of the centroid under different postures can be obtained. By means of the coordinate transformation relationship, the three-dimensional spatial coordinates of the centroid of the object can be accurately calculated.

Currently, the main methods for changing the posture of an object are rotation^[13,14] and inclination^[15,16]. Lin et al.^[17] designed a rotation angle measurement method based on three points, and used the response surface method to analyze the influence of random errors on measurement accuracy. Gu et al.^[18] proposed a three-point weighing method based on the principle of torque balance, and measured the centroid of the aircraft by rotating the aircraft

90°. Wu et al.^[19] used multiples of 90° of the sliding table rotation to change the posture and then calculated the centroid of the large-mass aircraft.

When traditional measurement methods encounter large-sized aircraft such as missiles and rockets that have fillings inside, large-angle tilting or rotation may pose safety risks. Therefore, this study combines existing measurement methods and proposes a centroid measurement method based on four-point support and small-angle tilting. By coordinate transformation, the gravity lines in two attitude product coordinate systems are obtained, and then the midpoint of the midline of the gravity action line is calculated, which is the product's centroid. Compared with traditional measurement methods, this method has a smaller tilt angle, improving overall safety. It does not have strict requirements for the initial position of the object to be measured, avoiding the influence of positioning errors on the measurement results. At the same time, this method introduces an intermediate coordinate system during measurement, reducing the number of product scans and key point coordinate calibration times, and improving the overall measurement efficiency.

1 Mass and centroid measurement methods

Under ideal conditions, it can be assumed that the gravitational field at which the object is located is uniform, and the centroid of the measured object coincides with the centroid. Therefore, by measuring the centroid of the object, its centroid can be determined. The main idea of this method is to separately measure the two gravity lines L_1 and L_2 passing through the centroid and in the same direction as it, under the two postures of the measured object, and to represent them in the measurement coordinate system. Then, by measuring the transformation relationship between the measurement coordinate system and the product coordinate system, L_1 and L_2 are represented in the product coordinate system. Finally, the intersection point of the two gravity lines is obtained, which can measure the centroid of the measured aircraft.

The specific flowchart is shown in Fig. 1. The establishment of each coordinate system and the mathematical model for calculating the centroid are elaborated below.

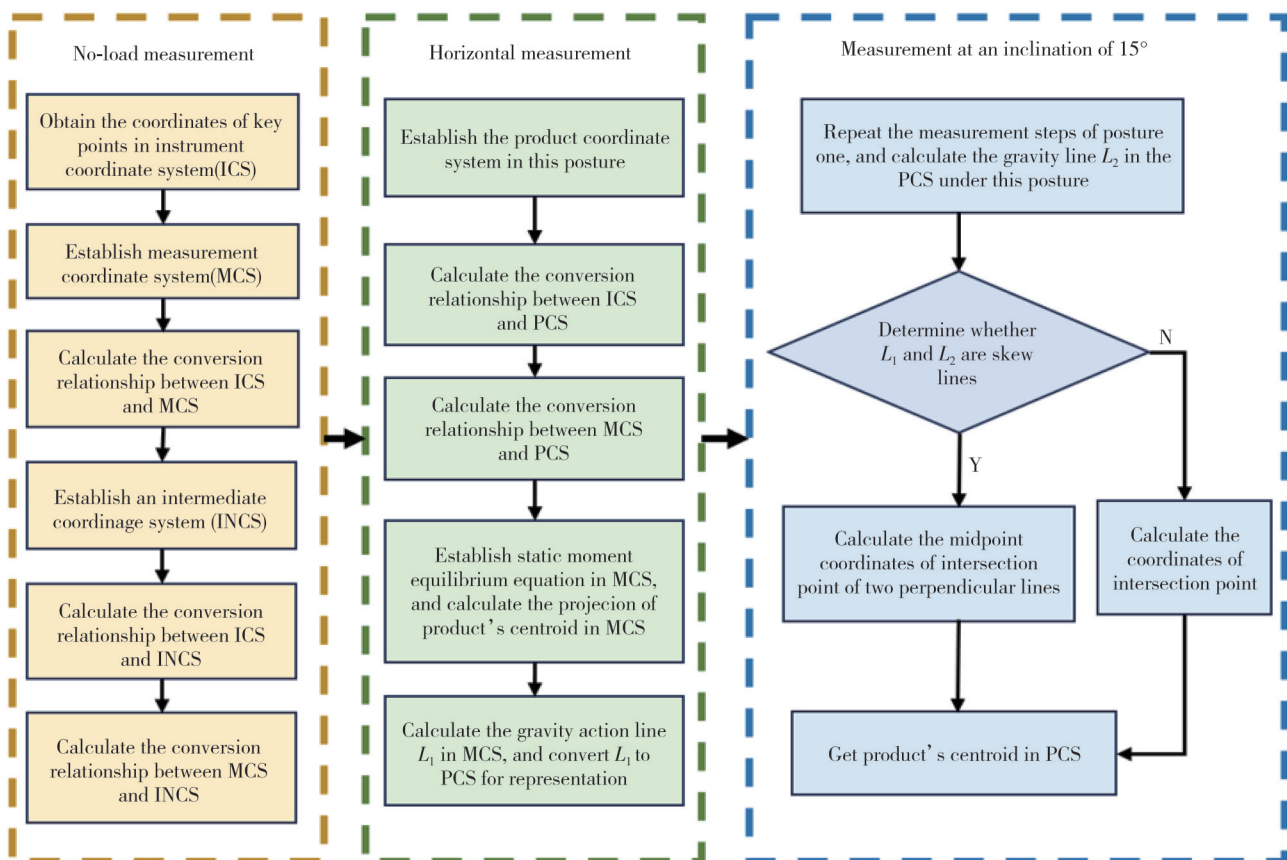


Fig. 1 Measurement flowchart

1.1 Establishment of coordinate systems

The key to centroid measurement lies in obtaining the intersection point of the gravity lines of the product to be measured under two different postures through coordinate system transformation. To determine the relative position relationship between the large aircraft and the measuring instrument, here the coordinate measurement of key points is carried out using a laser tracker, as shown in Table 1.

Table 1 Key point parameters

Parameter	Meanings
$S_i(X_{si}, Y_{si}, Z_{si}) (i=1, 2, 3, 4)$	Coordinates of four sensors in ICS
$T_i(X_{ti}, Y_{ti}, Z_{ti}) (i=1, 2, 3)$	Coordinates of three reference points in ICS
$K_i(X_{pi}, Y_{pi}, Z_{pi}) (i=1, 2, 3)$	Coordinates of three product reference points after loading the product
$M_{0j} (j=1, 2, 3, 4)$	Indicated values of each sensor when unloaded
$M_{ij} (i=1, 2) (j=1, 2, 3, 4)$	Indicated values of each sensor at attitude i

During the measurement process, four related coordinate systems need to be established.

1) Instrument coordinate system $O_1X_1Y_1Z_1$ (ICS). In order to establish the relationship among different coordinate systems, we introduce a laser tracker for measuring the coordinates of key points, and defines the reference coordinate system of the laser tracker as the ICS.

2) Measurement coordinate system $O_MX_MY_MZ_M$ (MCS). The plane P_M is fitted based on the coordinate data of four load cells. The geometric center of these sensors is taken as the origin O_M of MCS. The X_M axis points from the origin to the first sensor S_1 . The Z_M axis is perpendicular to the plane P_M and points upward. The direction of the Y_M axis is determined by the right-hand rule.

3) Intermediate coordinate system $O_{IN}X_{IN}Y_{IN}Z_{IN}$ (INCS). During the product measurement process, due to the obstruction caused by the upper auxiliary tooling and the measured component, it is impossible to directly measure the coordinates of the load cell. Therefore, it is not possible to directly calculate the conversion relationship between MCS and PCS. Thus, an intermediate coordinate system INCS needs to be introduced to indirectly calculate the conversion relationship. The INCS is determined by the reference points. Three reference points fit the plane P_{IN} . With T_1 as the origin, the X_{IN} axis points from the origin to the second reference point as T_2 , the Z_{IN} axis is perpendicular to the plane P_{IN} and points upwards, and the Y_{IN} axis is determined by the right-hand rule for its direction. The reference points are selected from the three typical positions around the base.

4) Product coordinate system $O_PX_PY_PZ_P$ (PCS). The

PCS is designated by the product designer and is established by measuring the coordinates of the product's reference points using a laser tracker. For ease of description, the product coordinate systems under the two measurement postures are denoted as $O_{P1}X_{P1}Y_{P1}Z_{P1}$ and $O_{P2}X_{P2}Y_{P2}Z_{P2}$, respectively. The final measurement results of the product's centroid are described in this coordinate system. The schematic diagram illustrating the establishment of key points of each coordinate system is shown in Fig.2.

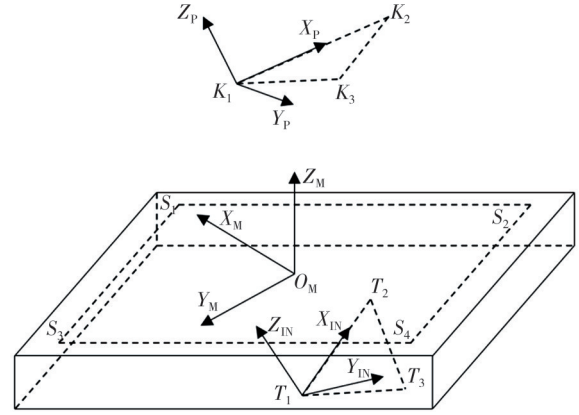


Fig. 2 Key points and schematic diagram of each coordinate system

1.2 Mass and centroid calculation model

Suppose there is a point in space, whose coordinates in the A coordinate system are (X_A, Y_A, Z_A) , and its coordinates in the B coordinate system are (X_B, Y_B, Z_B) . And the transformation matrix from the A coordinate system to the B coordinate system is T_{AB} . Then the relationship between the two sets of coordinates can be expressed by

$$\begin{bmatrix} X_A \\ Y_A \\ Z_A \\ 1 \end{bmatrix} = T_{AB}^{-1} \begin{bmatrix} X_B \\ Y_B \\ Z_B \\ 1 \end{bmatrix}, \tag{1}$$

$$T_{AB} = \begin{bmatrix} \mathbf{r}_{AB} & \mathbf{t}_{AB} \\ 0 & 1 \end{bmatrix}, \tag{2}$$

where \mathbf{r}_{AB} is the rotation matrix, representing the rotation from coordinate system A to coordinate system B; \mathbf{t}_{AB} is the translation vector, indicating the coordinates of the origin of coordinate system A in coordinate system B.

During the measurement process, the initial measurement result of the centroid is expressed in the coordinate system of the sensor, and ultimately needs to be converted to be expressed in the coordinate system of the object being measured. Taking the coordinate conversion process between the ICS and the MCS as an example.

During the coordinate transformation between the ICS and the MCS, as defined, it can be known that

$$\mathbf{t}_{AB} = \begin{bmatrix} \frac{\sum_{i=1}^4 X_{si}}{4} & \frac{\sum_{i=1}^4 Y_{si}}{4} & \frac{\sum_{i=1}^4 Z_{si}}{4} \end{bmatrix}^T, \quad (3)$$

$$\mathbf{r}_{AB} = [e_{X_M} \quad e_{Y_M} \quad e_{Z_M}]. \quad (4)$$

The direction vector of the X -axis of the MCS in the ICS is

$$\mathbf{D} = [X_{s1} \quad Y_{s1} \quad Z_{s1}]^T - \mathbf{t}_{AB}. \quad (5)$$

hen, the unit direction vector of the X -axis of the measurement coordinate system in the instrument coordinate system is

$$\mathbf{e}_{X_M} = \frac{\mathbf{D}}{|\mathbf{D}|}. \quad (6)$$

Plane P_M is derived by fitting four weighing sensors. Its equation is $ax + by + cz + D = 0$ (where \mathbf{D} can be any constant). Then

$$\begin{bmatrix} X_{s1} & Y_{s1} & Z_{s1} \\ X_{s2} & Y_{s2} & Z_{s2} \\ X_{s3} & Y_{s3} & Z_{s3} \\ X_{s4} & Y_{s4} & Z_{s4} \end{bmatrix} \begin{bmatrix} a \\ b \\ c \end{bmatrix} = \begin{bmatrix} -D \\ -D \\ -D \\ -D \end{bmatrix}. \quad (7)$$

$$\text{Let } \mathbf{M} = \begin{bmatrix} X_{s1} & Y_{s1} & Z_{s1} \\ X_{s2} & Y_{s2} & Z_{s2} \\ X_{s3} & Y_{s3} & Z_{s3} \\ X_{s4} & Y_{s4} & Z_{s4} \end{bmatrix}, \mathbf{B} = \begin{bmatrix} a \\ b \\ c \end{bmatrix}, \text{ and } \mathbf{N} = \begin{bmatrix} -D \\ -D \\ -D \\ -D \end{bmatrix},$$

then, the above expression can be rewritten as

$$\mathbf{M} \cdot \mathbf{B} = \mathbf{N}. \quad (8)$$

The value of \mathbf{B} can be obtained through the least squares method, which is the normal vector of the plane P_M , namely

$$x_{cg1} = \frac{(M_{11} - M_{01})X_1 + (M_{12} - M_{02})X_2 + (M_{13} - M_{03})X_3 + (M_{14} - M_{04})X_4}{(M_{11} - M_{01}) + (M_{12} - M_{02}) + (M_{13} - M_{03}) + (M_{14} - M_{04})}, \quad (14)$$

$$y_{cg1} = \frac{(M_{11} - M_{01})Y_1 + (M_{12} - M_{02})Y_2 + (M_{13} - M_{03})Y_3 + (M_{14} - M_{04})Y_4}{(M_{11} - M_{01}) + (M_{12} - M_{02}) + (M_{13} - M_{03}) + (M_{14} - M_{04})}. \quad (15)$$

Due to the vertical direction of the gravity line, the direction vector of the gravity line in the MCS is $(0, 0, 1)$. With the direction vector and a point on the line, the gravity line of the product in the MCS can be determined, and this gravity line is recorded as L_1 .

Based on the transformation matrix T_{MP1} between the MCS and the PCS, L_1 can be converted into an expression in the PCS. The coordinates $(x_{ocg1}, y_{ocg1}, z_{ocg1})$ of C_{G1} in the PCS and the direction vector (m_1, n_1, p_1) of the gravity line is expressed as

$$\begin{bmatrix} x_{cg1} & 0 \\ y_{cg1} & 0 \\ 0 & 1 \\ 1 & 1 \end{bmatrix} = T_{MP1}^{-1} \begin{bmatrix} x_{ocg1} & m_1 \\ y_{ocg1} & n_1 \\ z_{ocg1} & p_1 \\ 1 & 1 \end{bmatrix}. \quad (16)$$

$$\mathbf{B} = (\mathbf{M}^T \mathbf{M})^{-1} \mathbf{M}^T \mathbf{N}. \quad (9)$$

Then, the unit direction vector of the measurement coordinate system in the instrument coordinate system along the Z -axis is

$$\mathbf{e}_{Z_M} = \frac{\mathbf{B}}{|\mathbf{B}|}. \quad (10)$$

Finally, according to the right-hand rule, the unit direction vector \mathbf{e}_{Y_M} of the Y -axis in the measurement coordinate system can be obtained using

$$\mathbf{e}_{Y_M} = \mathbf{e}_{Z_M} \times \mathbf{e}_{X_M}. \quad (11)$$

At this point, the transformation matrix between the ICS and the MCS has been solved and is denoted as T_{IM} . Similarly, the transformation matrix T_{IIN} between the ICS and the INCS, as well as the transformation matrices T_{IP1} and T_{IP2} (postures 1 and 2) between the ICS and the PCS, can be obtained. Furthermore, the transformation matrix T_{MIN} between the MCS and the INCS can be calculated, and the transformation matrix T_{MP} between the MCS and the PCS under the current posture can also be determined.

$$T_{MINi} = T_{IIN}^{-1} T_{IPi}, \quad (i = 1, 2); \quad (12)$$

$$T_{MPi} = (T_{IIN}^{-1} T_{IM})^{-1} T_{MINi}, \quad (i = 1, 2). \quad (13)$$

Using the transformation matrix T_{IM} , the coordinates of the weighing sensor are converted from the ICS to the MCS, denoted as $S_i(X_i, Y_i, Z_i)$ ($i = 1, 2, 3, 4$). When the product is in posture 1, a static moment equilibrium equation is established in the MCS, thereby obtaining the projection of the product's centroid on the MCS's XOY plane, and this projection point is denoted as $C_{G1}: (x_{cg1}, y_{cg1}, 0)$.

The analytical expression of L_1 in the PCS is

$$\frac{x - x_{ocg1}}{m_1} = \frac{y - y_{ocg1}}{n_1} = \frac{z - z_{ocg1}}{p_1}. \quad (17)$$

The analytical expression of L_2 in the PCS is

$$\frac{x - x_{ocg2}}{m_2} = \frac{y - y_{ocg2}}{n_2} = \frac{z - z_{ocg2}}{p_2}. \quad (18)$$

Let the intersection point of the first line and the common perpendicular line be $C_1(X_1, Y_1, Z_1)$, and the intersection point of the second line and the common perpendicular line be $C_2(X_2, Y_2, Z_2)$. Then the most reliable coordinates of the centroid are the coordinates of the midpoint of these two intersection points. The intersection points C_1 and C_2 respectively satisfy

$$\begin{cases} (X_1 - X_2)m_1 + (Y_1 - Y_2)n_1 + (Z_1 - Z_2)p_1 = 0, \\ (X_1 - X_2)m_2 + (Y_1 - Y_2)n_2 + (Z_1 - Z_2)p_2 = 0, \end{cases} \quad (19)$$

$$\begin{cases} \frac{x - X_1}{m_1} = \frac{y - Y_1}{n_1} = \frac{z - Z_1}{p_1} = t_1, \\ \frac{x - X_2}{m_2} = \frac{y - Y_2}{n_2} = \frac{z - Z_2}{p_2} = t_2. \end{cases} \quad (20)$$

By solving simultaneously, the coordinates of C_1 and C_2 can be obtained. The midpoint of the line segment C_1C_2 is the coordinate of the centroid of the measured product. The coordinate of the centroid of the product in the PCS is

$$\begin{cases} x = \frac{X_1 + X_2}{2}, \\ y = \frac{Y_1 + Y_2}{2}, \\ z = \frac{Z_1 + Z_2}{2}. \end{cases} \quad (21)$$

The output values of the four sensors under the two postures and when the load is zero have been recorded. The mass M of the product can be obtained by taking the arithmetic mean of the net output values measured twice from the sensors as

$$M = \frac{\sum_{j=1}^4 (M_{1j} - M_{0j}) + \sum_{j=1}^4 (M_{2j} - M_{0j})}{2}. \quad (22)$$

2 Experiment

2.1 Mass and centroid measurement equipment

By adopting this method to design and complete a set of universal quality characteristic measurement system, both quality and three-dimensional centroid measurement can be achieved. The system measurement fixtures and internal structures are shown in Fig.3.

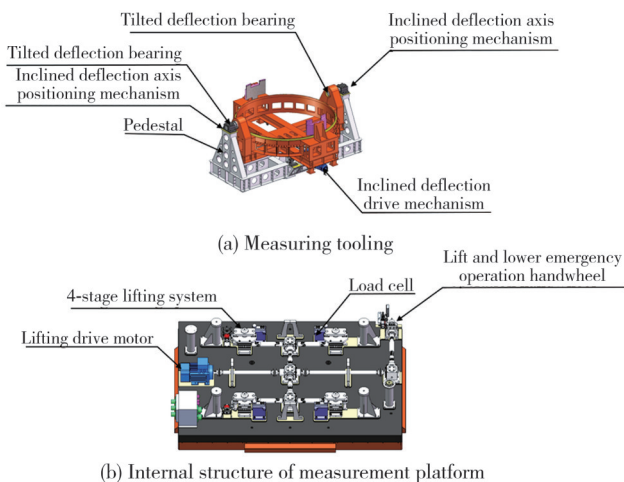


Fig. 3 Composition diagram of system

The system is divided into several parts: the quality characteristic measurement platform, the control platform, the supporting software, the measurement tooling that matches the interface of the measured product, and the standard sample, etc. The quality characteristic measurement platform mainly consists of the quality centroid measurement component (high-precision weighing sensor, auxiliary device, etc.), the adapter device, the base, the lifting system, and the peripheral partition of the measurement platform. The workpiece tooling designed for this system can be connected to the measured product (applicable to two different measurement states), and the data collection and calculation can be automatically completed through the computer, thereby achieving the measurement of the quality characteristic parameters of the product.

The physical diagram of the equipment is shown in Fig.4. The strength and deformation of the measurement platform directly affect the reliability and measurement accuracy of quality characteristic measurement. Therefore, it is necessary to analyze and verify the strength and deformation during the measurement process.



Fig. 4 Physical diagram of the equipment

Supposing the total weight of the product and the fixture on the measurement platform when fully loaded is 8 000 kg, during the measurement of the centroid, the finite element analysis results are shown in Fig.5.

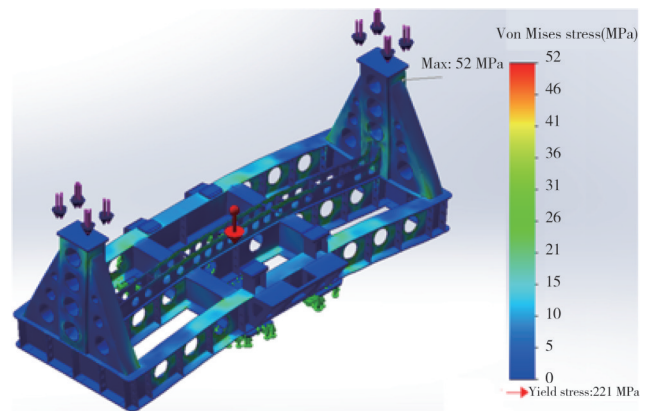


Fig. 5 Stress diagram

In Fig. 5, the maximum stress of the workpiece is $\sigma_{max}=52$ MPa, which meets the strength design requirements. In Fig. 6, the maximum deformation is

0.459 mm, which meets the precision requirements for the installation and positioning of the product in the measurement state.

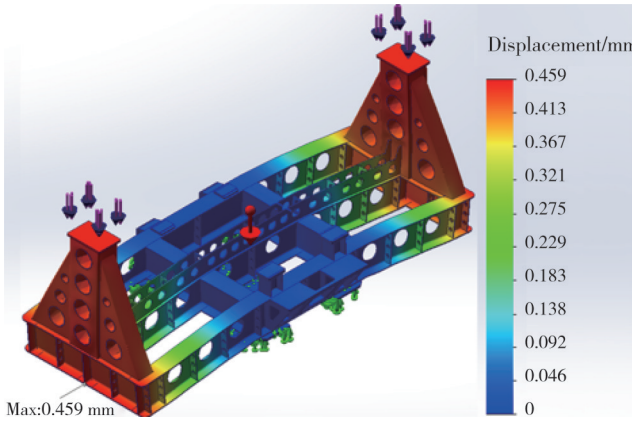


Fig. 6 Displacement diagram

In Fig. 7, the maximum stress in the workpiece is $\sigma_{\max}=41$ MPa, which meets the strength design requirements.

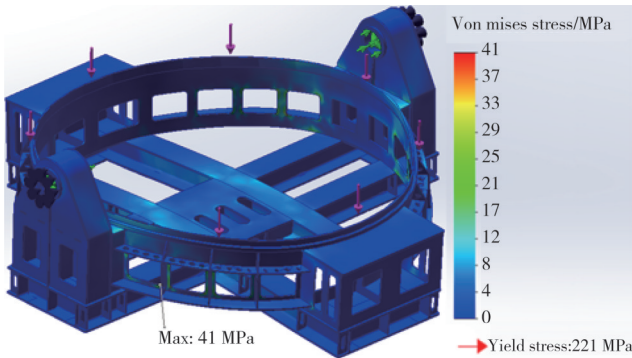


Fig. 7 Stress diagram

In Fig. 8, the maximum deformation is 0.361 mm, which meets the precision requirements for the installation and positioning of the product in the measurement state. The analysis results indicate that the design of the measurement fixture is reasonable and meets the requirements for measuring the quality characteristics.

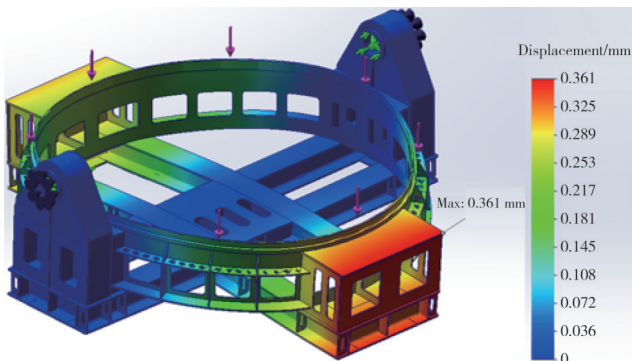


Fig. 8 Displacement diagram

2.2 Analysis of uncertainty in centroid measurement

2.2.1 Axial centroid uncertainty analysis

1) The influence of weighing sensor uncertainty on the axial coordinate of the centroid.

If the uncertainty of the weighing sensor is 0.01%, the influence of the uncertainty of the weighing unit on the axial centroid coordinates can be expressed as

$$\Delta x_c = \sqrt{\Delta x_1^2 + \Delta x_2^2 + \Delta x_3^2 + \Delta x_4^2} \approx 0.04 \text{ mm.} \quad (23)$$

2) The influence of sensor coordinate uncertainty on the axial coordinate of the centroid.

Before the measurement system was put into production, the coordinates of the sensor were determined using a laser tracker. The distance between the tracker and the weighing sensor was less than 5 m, and Δx_z can be regarded as 0.1 mm.

3) When the inclination angle is 15° , the influence of uncertain angle positioning on the axial coordinate of the centroid.

Ideally, the inclination angle should be fixed at 15° . However, due to processing and assembly errors, there is a certain deviation between the actual value and the ideal value. Using a laser tracker, this angle can be controlled within $30''$. According to Eq. (24), this influence is very small and can be almost ignored.

$$\Delta x_{\theta 1} = L(1 - \cos \theta) - L(1 - \cos(\theta - \theta')). \quad (24)$$

4) The influence of the uncertainty in the assembly tilt angle on the axial coordinate of the centroid.

The distance from the centroid to the end of the product is approximately $L=1000$ mm. Assuming the aircraft is not placed completely horizontally on the tabletop and has an inclination of θ_2 degrees, if $\theta_2=30''$, we have

$$\Delta x_{\theta 2} = L(1 - \cos \theta_2) = 0.1 \times 10^{-4} \text{ mm.} \quad (25)$$

5) The influence of other factors on the axial coordinate of the centroid is

$$\Delta x_Q = 0.1 \text{ mm.}$$

In conclusion, the uncertainty of the axial centroid of the aircraft is

$$\sigma_{x_{cg}} = \sqrt{\Delta x_c^2 + \Delta x_z^2 + \Delta x_{\theta 1}^2 + \Delta x_{\theta 2}^2 + \Delta x_Q^2} \approx 0.2 \text{ mm.} \quad (26)$$

The analysis of $\sigma_{y_{cg}}$ is the same as above.

2.2.2 Radial centroid uncertainty analysis

1) The influence of weighing sensor uncertainty on the radial coordinate of the centroid is

$$\Delta z_c = \sqrt{\Delta z_1^2 + \Delta z_2^2 + \Delta z_3^2 + \Delta z_4^2} \approx 0.04 \text{ mm.} \quad (27)$$

2) The influence of the coordinate uncertainty of the weighing sensor on the radial coordinate of the centroid is

$$\Delta z_z = 0.1 \text{ mm.}$$

3) The influence of the uncertainty of the aircraft's tilt angle on the radial coordinate of the centroid

If the installation accuracy can reach 0.04 mm, the inclination angle can be controlled at $\theta=10''$, then

$$\Delta z_\theta = L \times \sin \theta = 0.07 \text{ mm.} \quad (28)$$

4) The influence of other factors on the axial coordinate of the centroid is

$$\Delta z_Q = 0.05 \text{ mm.}$$

In conclusion, the uncertainty of the radial centroid of the aircraft is

$$\sigma_{z_r} = \sqrt{\Delta z_c^2 + \Delta z_z^2 + \Delta z_\theta^2 + \Delta z_Q^2} \approx 0.14 \text{ mm.} \quad (29)$$

2.2 Mass measurement experiment

In order to verify the quality measurement accuracy of this measurement system, standard components ranging from 3 500 kg to 4 400 kg were selected for testing. The quality test results are shown in Table 2.

The standard uncertainty can be estimated by the maximum error method. The calculation formula is

$$u = s = \frac{|\delta_i|_{\max}}{k_n}, \quad (30)$$

where u represents the standard uncertainty, s represents the standard deviation, δ_i represents the difference between an independent measurement value and the measured reference value, and k_n is the error method coefficient, which is related to the number of measurements n .

Table 2 Experimental data of mass testing

No.	True value/kg	Measurement value/kg	Error/kg
1	3 500.000	3 500.539	-0.539
2	3 600.000	3 600.590	-0.590
3	3 700.000	3 700.612	-0.612
4	3 800.000	3 799.604	0.396
5	3 900.000	3 900.370	-0.370
6	4 000.000	4 000.215	-0.215
7	4 100.000	4 099.793	0.207
8	4 200.000	4 200.028	-0.028
9	4 300.000	4 299.836	0.164
10	4 400.000	4 399.723	0.277

The expanded uncertainty with a 95% confidence level is

$$U_{95} = 2u. \quad (31)$$

Substituting the data in Table 2 into Eq. (30) and Eq. (31), the expanded uncertainty of the mass measurement of this system can be calculated as 0.77 kg. The maximum deviation of the quality test accuracy is 0.017%, which is less than 0.02%.

2.3 Centroid measurement experiment

To verify the centroid measurement accuracy of this system, centroid measurement experiments were conducted using standard parts. The measured workpiece and measurement postures are shown in Fig. 9, with posture 1 being placed horizontally and posture 2 being tilted at 15°. The test results are presented in Table 3.

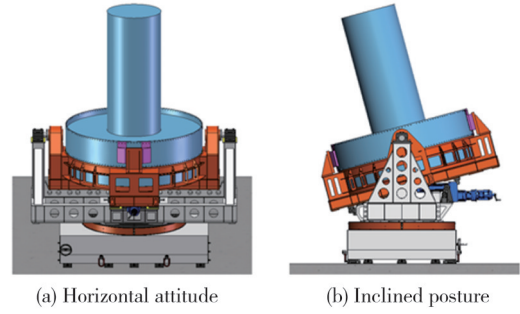


Fig. 9 Measurement postures

By analyzing the data in Table 3 and substituting it into Eq. (30) and Eq. (31), the maximum absolute error of the X-axis direction centroid measurement result of this system is 0.26 mm, with an expanded uncertainty of 0.15 mm; the maximum absolute error of the Y-axis direction centroid measurement result is 0.30 mm, with an expanded uncertainty of 0.21 mm; and the maximum absolute error of the Z-axis direction centroid measurement result is 0.23 mm, with an expanded uncertainty of 0.19 mm.

Table 3 Deviations of centroid measurements in each direction under two postures

Posture	No.	X-axis /mm	Y-axis /mm	Z-axis /mm
0°	1	-0.03	-0.25	0.17
	2	0.11	-0.05	0.23
	3	0.03	-0.18	0.08
15°	4	-0.17	0.30	-0.14
	5	0.07	0.03	0.03
	6	-0.26	0.14	-0.22

3 Conclusions

We design a system suitable for measuring the centroid of an aircraft. Firstly, the design principle of the system is elaborated in detail. By converting the coordinate system, the intersection point of the gravity lines is obtained, thereby obtaining the three-dimensional centroid of the aircraft. Then, the measurement accuracy of the system was tested using standard components. The experimental results show that the maximum deviation of the mass measurement accuracy of the system is less than 0.02%, the measurement accuracy of the centroid in the X-axis is

± 0.15 mm, the measurement accuracy of the centroid in the Y-axis is ± 0.21 mm, and the measurement accuracy of the centroid in the Z-axis is ± 0.19 mm, which meets the accuracy requirements of the system development.

Acknowledgement

This work was supported by National Natural Science Foundation of China-Youth Program (No. 62303420), and thank you to all the researchers who participated in this article for their hard work and contribution.

Declaration of conflicting interests

The authors have no conflict of interests related to this publication.

References

- [1] HE X, LI Z. A centroid measurement method based on 3D scanning. *Journal of Measurement Science and Instrumentation*, 2025, 16(2): 186-194.
- [2] YANG W P. Development trend of navigation guidance and control technology for new generation aircraft. *Acta Aeronautica et Astronautica Sinica*, 2024, 45(5): 529720.
- [3] WANG X J. Future development of space transportation system of China. *Missiles and Space Vehicles*, 2021(1): 1-6.
- [4] CHU W M, LI G, LI S G, et al. A centroid measurement method of large components for active compliant assembly. *Measurement*, 2024, 234: 114888.
- [5] LI Q, HUANG X C, ZHANG Z B, et al. Calibration method for mass and centroid measuring system of large launch vehicle. *Mechanical Engineering & Automation*, 2019(2): 5-7.
- [6] LI K, YANG L F, ZHENG F, et al. The research and practice of general measuring equipment. *China Quality*, 2024(7): 108-113.
- [7] ZHANG X L, WANG M B, TANG W Y, et al. A flexible measurement technique for testing the mass and center of gravity of large-sized objects. *Measurement Science and Technology*, 2020, 31(1): 015006.
- [8] ZHANG X L, YU H, TANG W Y, et al. General mass property measurement equipment for large-sized aircraft. *Sensors*, 2022, 22(10): 3912.
- [9] DAS R, FERDINAND CHRISTOPHER A. Accurate center of gravity measurement for aerospace components//*Advances in Automation, Signal Processing, Instrumentation, and Control*. Singapore: Springer Nature Singapore, 2021: 2557-2565.
- [10] CONG P T, TONG L, HAN H. Research of new centroid measurement system and method. *Tool Engineering*, 2015, 49(2): 86-89.
- [11] ZHANG X L, ZHANG L S, TANG W Y, et al. Research on flexible centroid measurement method for segments of large-thrust carrier rocket. *Applied Mechanics and Materials*, 2014, 597: 365-371.
- [12] MA C C, WANG J J, MA X, et al. Design of an automatic measuring device for mass center of mass based on multi-point weighing method. *Metrology & Measurement Technique*, 2024, 51(6): 53-56.
- [13] WANG J C. Research on the Integrated measuring technique of the mass properties for missile and rocket model. Chongqing: Chongqing University, 2018.
- [14] WANG K, LIU Z X, XING X F, et al. Development and research of measuring equipment for crash test dummy's center of mass and moment of inertia. *Journal of Machine Design*, 2025, 42(4): 156-161.
- [15] ZHANG Y H, FAN X H, ZHANG L Y, et al. The design and error analysis of a new mass and centroid measurement system for missiles based on four-point support approach. *Machine Design & Research*, 2016, 32(3): 96-99.
- [16] ZHAO X T, KANG J, LEI T Q, et al. Vehicle centroid measurement system based on forward tilt method error analysis. *IOP Conference Series: Materials Science and Engineering*, 2018, 452(4): 042189.
- [17] LIN C, ZHENG Y, GUANG C H, et al. Design implementation and error analysis of mass and centroid measurement of aircraft with wingspan. *Acta Aeronautica et Astronautica Sinica*, 2022, 43(1): 224893.
- [18] GU Q, LI B. A new three-point measurement method for mass, centroid and mass deviation of projectile. *Journal of Projectiles, Rockets, Missiles and Guidance*, 2005, 25(S9): 177-178.
- [19] WU B, WANG H F, MA G X. Measurement method of centroid for the vehicle with large mass. *Journal of Astronautic Metrology and Measurement*, 2007, 27(6): 28-30.

大型飞行器质量质心测量装置及方法研究

张晓琳^{1*}, 张煜杨¹, 杨利峰², 赵弘治², 王梅宝³

1. 哈尔滨工业大学 仪器科学与工程学院, 黑龙江 哈尔滨 150006;

2. 首都航天机械有限公司, 北京 100071;

3. 浙江理工大学 机械工程学院, 浙江 杭州 310018

摘要: 大型飞机质量特性参数的精确获取直接影响其性能特征。对于内部装填物的导弹和火箭等大型飞行器, 传统的大角度倾斜或旋转测量方法可能会带来安全风险。针对大型飞行器的特点, 结合现有测量方法, 设计了一种基于四点支撑和小角度倾斜测量的质量与质心测量方法, 并研制了一套质量、质心测试系统。该方法通过在两种姿态下进行坐标系变换获取产品坐标系下重力作用线的交点, 从而得到飞机的三维质心。文章首先详细阐述了该方法的原理, 然后介绍了设备的构成, 并分析了关键部件的结构应力, 最后进行了实验验证和不确定度分析。实验验证表明, 质量测量精度的最大偏差小于0.02%, 在X方向的质心测量精度为 ± 0.15 mm, 在Y方向为 ± 0.21 mm, 在Z方向为 ± 0.19 mm。

关键词: 大型飞行器; 质心测量; 坐标转换; 多点称重法; 重力线

引用格式: ZHANG Xiaolin, ZHANG Yuyang, YANG Lifeng, *et al.* Measurement device and method for mass and centroid of large aircraft. *Journal of Measurement Science and Instrumentation*, 2025, 16(3): 341-349. DOI: 10.62756/jmsi.1674-8042.2025033